Dynamics of acoustically-induced boundary-layer flashbacks in a dump combustor

Jean-Michel Klein[a], Aurelien Genot[b], Axel Vincent-Randonnier[c], and Arnaud Mura[d]
[a]Barcelona Supercomputing Center (BSC), Plaza Eusebi Güell, Barcelona, 1-3, 08034, Spain
[b]DMPE, ONERA, Université de Toulouse, 31000, Toulouse, France
[c]DMPE, ONERA, Université de Toulouse, 31410, Mauzac, France
[d]Pprime UPR 3346 CNRS ENSMA, and University of Poitiers, F-86961, Poitiers, France

1 Introduction

Flame flashback, the upstream propagation of the flame front, is a common cause of burner failure or damage due to combustion instabilities [1, 2]. Although combustion instabilities and flame response remain the subject of active research [3], studies of periodic flashback dynamics are limited. The present work focuses on boundary layer flashbacks — where the flame propagates upstream at the vicinity of the combustor walls, in regions with low flow velocities [1] — driven periodically by the combustor acoustics. Several 2D numerical simulations of unstable dump combustors [4] are analyzed, emphasizing periodic oscillations within the boundary layers influenced by the flame.

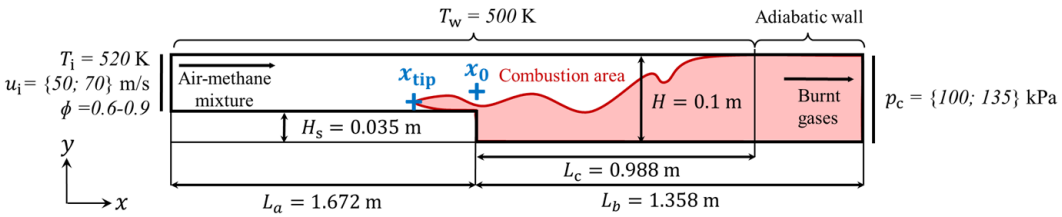

Figure 1: Sketch of the computational domain. Definition of points $\boldsymbol{x_0} = [0, 0.015]$ m (coreflow), and $\boldsymbol{x_{tip}}$ (flame tip).

2 Description of the numerical dataset

Figure 1 shows the computational domain retained for the purpose of this study. A backward-facing step (BFS) of height $H_s = 0.035$ m splits the duct into 2 domains with respective lengths $L_a = 1.672$ m, $L_b = 1.358$ m. The right duct height is $H = 0.1$ m. Seven numerical simulations are analyzed, featuring a premixed methane-air mixture injected at $T_i = 520$ K, with inlet velocities u_i of 50 or 70 $\mathrm{m \cdot s^{-1}}$ and equivalence ratios Φ ranging from 0.6 to 0.9. The imposed outlet pressure p_c is 100.4 or 135 kPa. Wall cooling is modeled with an imposed wall temperature $T_w = 500$ K in combustion zones. The Large-Eddy Simulations (LES) framework is applied with the WALE subgrid scale model [5] [1]. A single-step chemistry and the thickened flame approach capture the effects of turbulence on combustion.

[1]The description of the numerical modeling being here very brief for the sake of conciseness, the reader is however referred to reference [4] where further details are provided.

The 2D domain is meshed with $450,000$ triangular and quadrilateral elements, refined near the step with a characteristic cell size of 400 μm. The boundary layer mesh resolution allows the accurate capture of dynamic phenomena. At this level, it is important to acknowledge that performing 2D simulations within the LES framework may appear inadequate, as turbulent eddies are not well represented in such simulations. However, in this study, turbulence is not the primary phenomenon of interest, and the focus is on acoustically induced oscillations. In this regard, 2D numerical simulations offer a practical advantage, enabling a more extensive parametric study due to their lower computational cost.

To differentiate the different simulations, the nomenclature S/U-p_c-u_i-Φ is used. S/U designates stable (S) and unstable (U) cases and p_c is the operating pressure in kPa. It should be emphasized that stable operating conditions are reached by adding a large plenum to the outlet, thus evacuating the acoustic energy from the combustor.

3 Parametric study analyses

For *unstable cases*, the set of boundary conditions favors the onset of quarter-wave acoustic modes [3], which cause significant flow velocity oscillations, leading to two types of periodic flame flashbacks: *(i)* coreflow flashback, where the bulk flow velocity $u(\boldsymbol{x_0})$ reverts at the vicinity of the step, causing massive flame motions toward the inlet; and *(ii)* boundary layer flashbacks, in which the flame locally propagates upstream in the boundary layer. The first one features couplings between shedded vortices, flow recirculation, flame motions, and acoustics. A detailed description of this mechanism is given in reference [4]. The second mechanism, which is dominant in most of the seven cases studied here, is investigated hereafter.

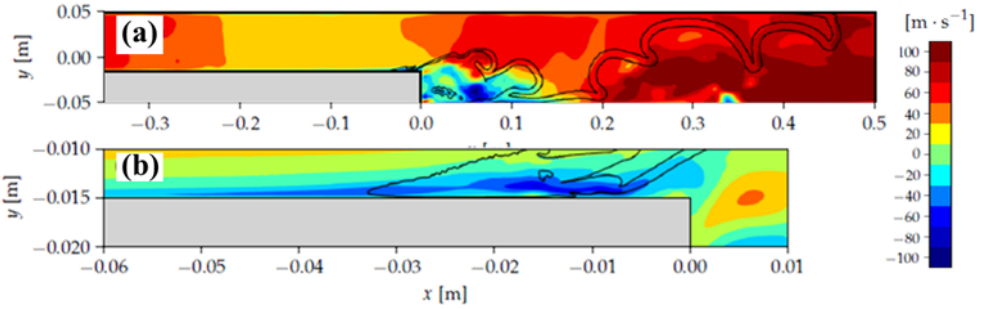

Figure 2: Instantaneous velocity fields with heat-release rate isolines (10^7 W $\cdot$ m^{-3}) during a (a) flashback event for the U-135-50-0.8 simulation case with (b) a zoom in the boundary layer.

Figure 2.a displays a snapshot with an event of boundary layer flashback in case U-135-50-0.8 (unstable case with an operating pressure of 135 kPa, a mean bulk flow velocity of 50 m $\cdot$ s^{-1} and an equivalence ratio of 0.8). A zoom on the boundary layer (Fig. 2.b) shows that the flame, the presence of which is revealed by the black isoline, gives rise to the detachment of the boundary layer and triggers local flow reversal.

Several quantities related to the boundary layer flashback have been evaluated, and table 1 presents key statistics for each case. The second column reports the mean axial velocity $u_0(\boldsymbol{x_0})$ and its fluctuation $u_1^{\mathrm{RMS}}(\boldsymbol{x_0})$ (standard deviation) at position $\boldsymbol{x_0}$ (center of the duct at the step location, see Fig. 1). The third column quantifies flashbacks with the length $\ell_{\mathrm{fb}} = |x_{\mathrm{tip},0} - x_{\mathrm{tip},1}^{\mathrm{RMS}}|$. The quantity x_{tip} denotes the axial position of the point located in the flame front ($\dot{q} > 10^7$) which is the furthest upstream. Thus, ℓ_{fb} quantifies its standard deviation subtracted from its mean value.

Table 1: Statistics on the occurence of flashback events

Computed case	$u_0(\boldsymbol{x_0}) \pm u_1^{\mathrm{RMS}}(\boldsymbol{x_0})$	$\ell_{\mathrm{fb}}/H_{\mathrm{s}}$	$\mathbb{P}\left(x_{\mathrm{tip}} < 0\right)$	$\mathbb{P}\left(u_{\mathrm{tip}} < 0\right)$	$f_{\mathbf{fb}}$	$f_{\mathbf{bo}}$
S-100-50-0.8	$50 \pm 4\ \mathrm{m \cdot s^{-1}}$	0.03	0.02	0.43	716 Hz	66 Hz
U-100-50-0.6	$50 \pm 56\ \mathrm{m \cdot s^{-1}}$	1.06	0.62	0.57	845 Hz	367 Hz
U-100-50-0.7	$50 \pm 25\ \mathrm{m \cdot s^{-1}}$	1.28	0.63	0.53	744 Hz	333 Hz
U-100-50-0.8	$50 \pm 17\ \mathrm{m \cdot s^{-1}}$	0.83	0.78	0.55	611 Hz	333 Hz
U-100-50-0.9	$50 \pm 27\ \mathrm{m \cdot s^{-1}}$	2.17	0.73	0.53	589 Hz	266 Hz
U-135-50-0.8	$50 \pm 24\ \mathrm{m \cdot s^{-1}}$	1.85	0.77	0.51	567 Hz	222 Hz
U-135-70-0.8	$70 \pm 49\ \mathrm{m \cdot s^{-1}}$	1.88	0.75	0.53	711 Hz	311 Hz

From now on, the authors specify that what is hereafter referred to as a "flashback event" corresponds to a continuous interval of time over which x_{tip} and $u_{\mathrm{tip}} = \partial x_{\mathrm{tip}}/\partial t$ are simultaneously negative, *i.e.* when the flame propagates upstream. The probabilities $\mathbb{P}(x_{\mathrm{tip}} < 0)$ and $\mathbb{P}(u_{\mathrm{tip}} < 0)$ (fourth and fifth columns) thus indicate the fraction of time for which the flame is upstream from the step edge and propagates reversely to the average flow. Finally, the last two columns gather the frequencies f_{fb} and f_{bo}, representing the rate of velocity reversals (flashback events) and the frequency relevant to negative values of x_{tip}, respectively. The first line of table 1 indeed shows that, for the *stable case*, where no acoustic oscillations are present, ℓ_{fb} is significantly lower than for the *unstable cases*, *i.e.* the flashback events are marginal.

Flashbacks occur when the flow velocity locally drops below the flame propagation velocity, and several studies suggest examining velocity fluctuations upstream to assess flashback propensity [2, 6, 7]. In this study, the increase in flashback intensity (length ℓ_{fb}) correlates somewhat with $u_0(\boldsymbol{x_0}) \pm u_1^{\mathrm{RMS}}(\boldsymbol{x_0})$. Indeed, ℓ_{fb} successively increases in the *unstable cases* U-100-50-0.8, U-100-50-0.7, U-100-50-0.9, and U-135-50-0.8 which are characterized by successive increases in velocity fluctuations. However, cases U-100-50-0.6 and U-135-50-0.8 show that higher velocity fluctuations do not always correlate with a significant increase in ℓ_{fb}. However, ℓ_{fb} seems to correlate well with f_{fb}. For instance, in cases U-100-50-0.7, U-100-50-0.9, and U-135-50-0.8, with similar velocity fluctuations ($u_1^{\mathrm{RMS}}(\boldsymbol{x_0}) = 24 - 27\ \mathrm{m \cdot s^{-1}}$), ℓ_{fb} is larger for the last two cases, which feature lower f_{fb}. It is also interesting to note that f_{bo} is always significantly lower than f_{fb}, which means that, after the flame initially propagates upstream ($u_{\mathrm{tip}} < 0$ and $x_{\mathrm{tip}} < 0$) due to an initial flashback, a series of "secondary" flashbacks occur before the flame temporarily restabilizes downstream of the step ($x_{\mathrm{tip}} > 0$).

Table 2: Quantification of flame-wall interactions during flashbacks

Computed case	$\langle s_{\mathrm{tip}} \rangle$	$\langle \delta_{\mathrm{q}} \rangle$	$\mathcal{G}_{\mathrm{c}}$
S-100-50-0.8	$0.39\ \mathrm{m \cdot s^{-1}}$	0.32 mm	$1218\ \mathrm{s^{-1}}$
U-100-50-0.6	$5.26\ \mathrm{m \cdot s^{-1}}$	1.90 mm	$2768\ \mathrm{s^{-1}}$
U-100-50-0.7	$5.64\ \mathrm{m \cdot s^{-1}}$	0.73 mm	$7726\ \mathrm{s^{-1}}$
U-100-50-0.8	$4.62\ \mathrm{m \cdot s^{-1}}$	0.60 mm	$7830\ \mathrm{s^{-1}}$
U-100-50-0.9	$4.16\ \mathrm{m \cdot s^{-1}}$	0.89 mm	$4674\ \mathrm{s^{-1}}$
U-135-50-0.8	$3.24\ \mathrm{m \cdot s^{-1}}$	0.76 mm	$4263\ \mathrm{s^{-1}}$
U-135-70-0.8	$3.97\ \mathrm{m \cdot s^{-1}}$	1.14 mm	$3482\ \mathrm{s^{-1}}$

To complete the analysis, the time-averaged value $\langle s_{\mathrm{tip}} \rangle$ of the flame tip propagation speed $s_{\mathrm{tip}} = u_{\mathrm{tip}} - u(\mathrm{x_{tip}})$ studied in the context of boundary layer flashbacks is also estimated [1, 9] and reported in table 2. For the *stable case* S-100-50-0.8, this speed is one order of magnitude below those observed in the *unstable cases*. It agrees with the literature reporting one order of magnitude faster flames when confined [1]. Indeed, the probability $\mathbb{P}(x_{\mathrm{tip}} < 0)$ is almost zero for the *stable case* and exceeds 0.62 for

the *unstable cases* (see Table 1), indicating that, in the latter, the flame remains predominantly confined within the boundary layers. The quenching distance $\langle \delta_{\rm q} \rangle$, *i.e.*, average distance between the flame and the bottom wall during flashback events, and the critical velocity gradient $\mathcal{G}_{\rm c} = \langle s_{\rm tip} \rangle / \langle \delta_{\rm q} \rangle$ are also reported in table 2. Although the critical velocity gradient has been extensively used in the literature to evaluate or predict flashback propensity [1], no evident correlation with $\ell_{\rm fb}$ can be found in the present study. This suggests that *(i)* unsteady flame and flow features such as the statistics presented in table 1 should be accounted in the description of these flashback events; *(ii)* it might be possible to derive new dimensionless numbers allowing to describe their propensity; and that *(iii)* their phenomenology should be further investigated.

4 Focus on the axial velocity behavior

The flashback dynamics is now studied with the help of the axial velocity equation, whose various terms have been estimated from the numerical dataset:

$$\frac{\partial u}{\partial t} = \underbrace{-u\frac{\partial u}{\partial x}}_{\mathcal{S}_{\mathrm{adv},x}} \underbrace{-v\frac{\partial u}{\partial y}}_{\mathcal{S}_{\mathrm{adv},y}} \underbrace{-\frac{1}{\rho_0}\frac{\partial p}{\partial x}}_{\mathcal{S}_{\mathrm{ac}}} \underbrace{-\left(\frac{1}{\rho}-\frac{1}{\rho_0}\right)\frac{\partial p}{\partial x}}_{\mathcal{S}_{\rho}} \underbrace{+\left(\frac{1}{\rho}\boldsymbol{\nabla}\cdot[\boldsymbol{\tau}]\right)\cdot\boldsymbol{e_x}}_{\mathcal{S}_{\mu}} \underbrace{+\left(\frac{1}{\rho}\boldsymbol{\nabla}\cdot[\boldsymbol{\tau}^{\mathbf{SGS}}]\right)\cdot\boldsymbol{e_x}}_{\mathcal{S}_{\mathrm{SGS}}} \quad (1)$$

The first two terms ($\mathcal{S}_{\mathrm{adv},x}$ and $\mathcal{S}_{\mathrm{adv},y}$) represent advection induced by velocity components along directions x and y, respectively. The pressure gradient term $(-(1/\rho)\partial p/\partial x)$ is decomposed into: *(i)* ($\mathcal{S}_{\mathrm{ac}}$), which captures pressure variations (mainly caused by the acoustics) over time, excluding density changes; and *(ii)* $\mathcal{S}_{\rho}$, which accounts for density variations, (including flame-induced temperature variations). The term $\mathcal{S}_{\mu}$ evaluates viscous forces. The term $\mathcal{S}_{\mathrm{SGS}}$ captures the effect of subgrid-scale viscosity. Since periodic phenomena are studied, applying a Discrete Fourier Transform (DFT) on this equation allows to derive an equation for the axial velocity fluctuations $\hat{u}$ in the frequency domain:

$$\hat{u}(f) = \widehat{u_{\mathrm{adv},x}}(f) + \widehat{u_{\mathrm{adv},y}}(f) + \widehat{u_{\mathrm{ac}}}(f) + \widehat{u_{\rho}}(f) + \widehat{u_{\mu}}(f) + \widehat{u_{\mathrm{SGS}}}(f) \quad (2)$$

where $\hat{u}_{\mathcal{S}}(f) = \widehat{\mathcal{S}}(f)/(-i2\pi f)$ for a given source term $\mathcal{S}$ evaluated at any given frequency f.

Since the flame and flow dynamics are essentially driven by the excited acoustic modes [4], the terms of equation (2) have been computed on the whole datasets at their eigenfrequencies $f_{(2n-1)/4}$, where n is the mode number. The case U-100-50-0.9 has first been selected to analyze these source terms because it is the one featuring the most violent flashback events ($\ell_{\rm fb}$ is the highest for this case, see Tab. 1) and figure 3 shows these source terms oscillations at the frequency $f_{5/4} = 210$ Hz of the third acoustic mode (five-quarter wave mode), which is, in this case, the dominant one. $\widehat{u_{\mathrm{SGS}}}(f)$ is the only negligible term and is therefore not shown. The real parts of those terms are displayed for various phases along the y axis at abscissa $x = -H_{\rm s}/2$, which is close to the step and where the flame periodically propagates in the boundary layer. Figure 3.e also shows fluctuations of the flame tip position and of the coreflow velocity ($\hat{u}(\boldsymbol{x_0})$) at the same frequency.

It can be seen that phase $\theta = 0$ (Fig. 3.a) corresponds to the time where the axial velocity is maximal, see Fig. 3.e. Close to the walls, the axial velocity uniformity breaks due to viscous forces and advection terms ($\mathrm{Re}(\widehat{u_{\mu}})$ and $\mathrm{Re}(\widehat{u_{\mathrm{adv},x}})$), which are in phase opposition with the acoustic term $\mathrm{Re}(\widehat{u_{\mathrm{ac}}})$. At phase $\theta = \pi/2$ (Fig. 3.b), the coreflow velocity is near zero as $\mathrm{Re}(\widehat{u_{\mathrm{ac}}})$ nullifies. The decrease of $\mathrm{Re}(\widehat{x_{\mathrm{tip}}})$ indicates that the flashback is initiated. Local velocity inversion occurs near the boundary layers, influenced by viscous forces ($\mathrm{Re}(\widehat{u_{\mu}})$) and advection ($\mathrm{Re}(\widehat{u_{\mathrm{adv},x}})$), which extends this inversion above the quenching point. The axial velocity is minimal for phase $\theta = \pi$ (Fig. 3.c). The real part

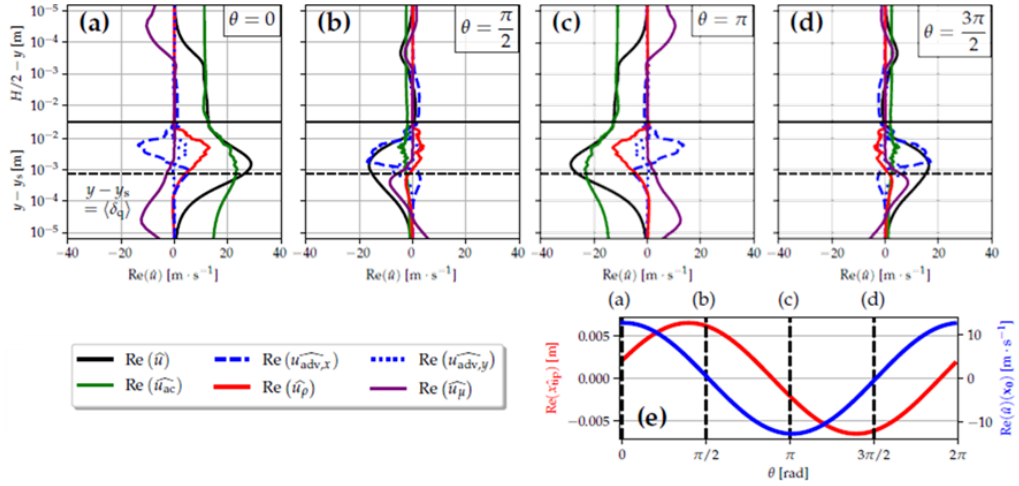

Figure 3: Real part of the Fourier transforms of the terms of equation (1) plotted for the frequency $f_{5/4}$ and along the line $x = -H_s/2$ for different phases (a-d) for case U-100-50-0.9. The evolution of the real part of $\widehat{x_{tip}}$ as well as the velocity $\hat{u}(\boldsymbol{x_0})$ is also plotted for these same phases (e). The phase $\theta = 0$ corresponds to the moment when, for the frequency $f_{5/4}$, the axial velocity reaches its maximum at the step. Dashed lines also report the quenching point in (a-d).

$\mathrm{Re}(\widehat{u_{ac}})$ is also minimum after the change of sign, causing full velocity inversion, with a local minimum near the quenching point due to thermal expansion effects. The flashback finally ends when $\theta = 3\pi/2$ (Fig. 3.d), while $\mathrm{Re}(\widehat{x_{tip}})$ increases back. The velocity becomes positive again, with a phase advance near the walls. Actually, flashback occurs for $\pi/2$ (Fig. 3.b), when the axial velocity fluctuation — despite being nul in the coreflow — locally reverses in the boundary layers, due to the contributions of viscous stress and advection. Similar analyses performed on the six other computed case, in flow regions located further upstream (where the flame does not propagate), and at other eigenfrequencies also lead to the following statements. First, the absence of the flame leads to a dynamics similar to what can be seen in the above parts (*i.e.* close to the top wall) of figures 3.a-d, *i.e.* less significant velocity reversal due to the vanishing contributions of the terms $\mathrm{Re}(\widehat{u_\rho})$ and $\mathrm{Re}(\widehat{u_{\mathrm{adv},x}})$ (flame-induced density variations and advection) and slightly lower viscous forces. Second, the same phenomenology is observed at each eigenmode frequency, except $f_{1/4} = 60$ Hz (first acoustic mode). At this frequency, the flashback starts before the local velocity being reversed, and the reversal is then triggered by a combination of the acoustics ($\mathrm{Re}(\widehat{u_{ac}})$) and, mostly, the density variations ($\mathrm{Re}(\widehat{u_\rho})$) induced by the flame. This second flashback scenario (for $f_{1/4}$) might seem easier to interpretate than the one described above, since the flame front having a propagation velocity (s_{tip}, see table 2), it should start propagating upstream before the flow reverts.

Although flow reversal and flame propagation, in general, depend on the summation of the contributions of each individual acoustic mode, and are therefore rather difficult to interpretate in such cases, two main tendencies relevant to boundary layer flashback dynamics can, however, be highlighted:

- At lower frequencies (typically $f_{1/4}$), flashback is directly initiated by the flame propagation, and flow reversal is then favored by the density fluctuations directly caused by the flame.
- At higher frequencies (typically $f_{5/4}$), flow reversal tends to be indirecly triggered by the flame, through a combination of advection and increased viscosity, which then triggers new flashbacks.

These statements makes sense insofar as the values of f_{fb} reported in table 1 are higher than the individual eigenfrequencies and as f_{bo} is lower than f_{fb}. Indeed, this suggests that when a flame flashback is

initially triggered at a lower frequency, several "secondary" flashbacks then occur at higher frequencies through the mechanisms described above.

5 Conclusion

With the purpose of understanding acoustically-induced boundary-layer flashbacks, a database of dump combustor simulations has been investigated. Quantities used to describe the flashback propensity of steady flames (quenching distances, critical velocity gradients) have been evaluated. They fail to adequately describe the propensity to periodic flashbacks and other quantities, such as the amplitude of velocity oscillations, or the flashback frequencies should be taken into account. Furthermore, the analysis of the velocity equation terms has clarified the associated phenomenology: at low frequency, flow reversal might follow flashbacks due to the flame-induced density variations, and at higher frequencies, flow reversal is favored by a combination of flame-amplified viscous forces and advection, and might cause new flashbacks. Times lags between flame-induced thermal expansion and convection might also have some influence.

Those findings improve our understanding of periodic flame flashbacks and can be useful to develop future dynamic models, allowing to predict the propensity to flashbacks. The analysis of source terms performed in section 3 could also help derive new dimensionless numbers associated with the quantities (analyzed in section 2), which describe periodic flashback propensity.

References

[1] Kalantari A, McDonell V (2017). Boundary layer flashback of non-swirling premixed flames: Mechanisms, fundamental research, and recent advances. Prog. Energ. Combust, 61: 249-292

[2] Boulal S, Genot A, Klein J-M, Fabignon Y, Vincent-Randonnier A, Sabelnikov V (2023). On the hydro-acoustic coupling responsible for the flashback limit-cycle of a premixed flame at a backward-facing step. Combust. Flame, 257(2): 112999

[3] Schuller T, Poinsot T, Candel S (2020). Dynamics and control of premixed combustion systems based on flame transfer and describing functions. J. Fluid. Mech, 894: P1

[4] Klein J-M, Genot A, Vincent-Randonnier A, Mura A (2022). Combustion thermoacoustics: on the relevance of some stability criteria. EUCASS-3AF

[5] Sagaut P (2006). Large eddy simulation for incompressible flows: an introduction. Springer Science & Business Media

[6] Altay HM, Speth RL, Hudgins DE, Ghoniem AF (2009). Flame–vortex interaction driven combustion dynamics in a backward-facing step combustor. Combust. Flame, 156(5): 1111-1125

[7] Hong S, Speth RL, Shanbhogue SJ, Ghoniem AF (2013). Examining flow-flame interaction and the characteristic stretch rate in vortex-driven combustion dynamics using PIV and numerical simulation. Combust. Flame, 160(8): 1381-1397

[8] Hoferichter V, Sattelmayer T (2018). Boundary layer flashback in premixed hydrogen–air flames with acoustic excitation. Journal of Engineering for Gas Turbines and Power. J. Eng. Gas Turb. Power, 140(5): 051502

[9] Lewis B, Von Elbe G (1943). Stability and structure of burner flames. J. Chem. Phys, 11: 75–97